Stress Fluctuations in a 2D Granular Couette Experiment: A Continuous Transition

Daniel Howell and R. P. Behringer

*Department of Physics and Center for Nonlinear and Complex Systems, Duke University,
Durham, North Carolina 27708-0305*

Christian Veje

Niels Bohr Institute, Copenhagen, Denmark
(Received 6 October 1998)

Experiments on a slowly sheared 2D granular material show a continuous transition as the packing fraction γ passes through $\gamma_c \simeq 0.776$. The mean stress, $\bar{\sigma}$, plays the role of an order parameter. As $\gamma \to \gamma_c$ from above, (1) the compressibility becomes large, (2) a slowing down of the mean velocity occurs, (3) the force distributions change, and (4) the network of stress chains changes from intermittent long radial chains near γ_c to a tangled dense network for larger γ. [S0031-9007(99)09490-9]

Granular systems have captured much recent interest because of their rich phenomenology and important applications [1]. Even in the absence of strong spatial disorder of the grains, static arrays show inhomogeneous spatial stress profiles called stress chains [2], where forces are carried primarily by a small fraction of the total number of grains (see Fig. 1). Under slow deformation, changes in the stress chains lead to strong temporal fluctuations [3,4]. We will focus here on such a slowly driven system, Couette shear flow in 2D, on a size scale where stress chains play an important role.

There are two concepts that are particularly relevant to slow shearing: Reynolds dilatancy and Coulomb friction. If shear is applied to a densely packed sample of hard frictional grains, the system must dilate (Reynolds dilatancy) so the grains can move around each other [5]. Under continued shearing, the dilation and displacement of grains is typically limited to a region that is ∼5–10 grains wide called a shear band. Coulomb friction is indeterminate for an arbitrary static rigid granular array, leading to randomness/history dependence. The challenge is then to relate control parameters and possibly history to the statistical and mean properties of the system.

Several recent theoretical works [6–8] have provided a context for understanding static stress distributions in granular materials. The first of these, the q model [6], predicts a force distribution for static systems $P(F) \propto F^{N-1} \exp(-F/F_o)$, where N is the system dimension. This model is based on a regular array of grains, neglects torques, and considers the force balance in one direction only. It introduces randomness by assuming that the force on a grain in one layer is balanced by transmitting fractions q and $1 - q$ to the two supporting grains of an ordered dense packing (assuming a 2D system) in the next layer, where q is a random number uniformly distributed in $0 \leq q \leq 1$. Various other lattice models [7] contain features that guarantee torque and vector force balance, the possibility of correlated stress chains, or other features

of random packing. An alternative approach, contact dynamics [8], is a scheme to resolve the indeterminacy of static Coulomb friction. This model also predicts $P(F) \propto \exp(-F/F_o)$ for large forces.

We have carried out experiments on a 2D "granular" system consisting of photoelastic (i.e., birefringent under strain) polymer disks [9] subject to steady slow shearing in a flat Couette geometry. By viewing the disks through an arrangement of circular polarizers, it is possible to characterize the stress on the disks using photoelasticity [10]. (We have reported velocity and disk rotation data
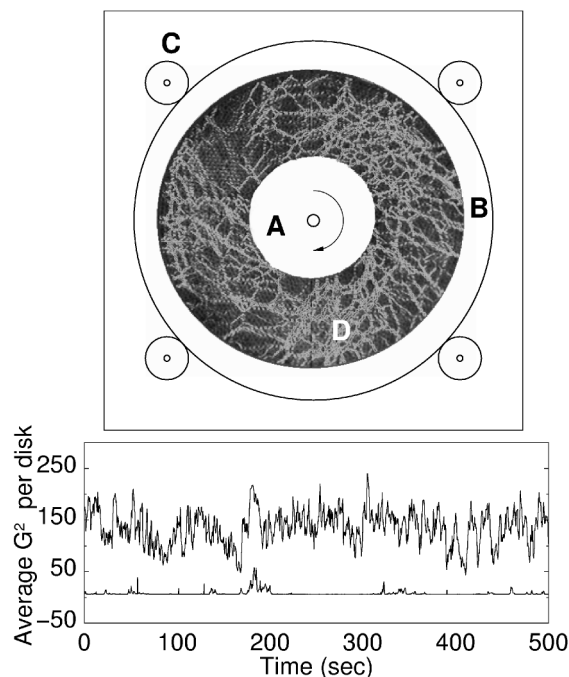

FIG. 1. Top: image of stress chains from the present experiment using photoelasticity overlaid on a schematic of the apparatus. Bottom: representative time series for stress fluctuations integrated over ∼1/10 of the disks. The lower trace is just above γ_c at $\gamma = 0.777$, and the upper trace has $\gamma = 0.803$.

elsewhere [11].) For slow shearing, we would expect that the grains are almost always near a state of static equilibrium. Thus, the experiment produces an ensemble of nearly steady states of similar history to which we might compare the models discussed above.

A key finding of this work is the identification of a continuous transition in the dynamical behavior as the fraction of area occupied by disks, or packing fraction, γ, approaches $\gamma_c \simeq 0.776$ from above $(\gamma \rightarrow \gamma_c^+)$. Thus, γ corresponds to the packing fraction at which grains or disks in this 2D system just maintain frictional contact; γ_c (which is likely to be system dependent) is close to the packing fraction for a square lattice, $\gamma_s = \pi/4 \simeq 0.785$, and below the random close packing value, $\gamma \simeq 0.82$. As $\gamma \rightarrow \gamma_c^+$, all components of the stress, σ, vanish. Hence, σ serves as an order parameter, and $\gamma - \gamma_c$ measures the distance from the transition, which we refer to as the strengthening (or softening) transition (ST). As $\gamma \rightarrow \gamma_c^+$, fluctuations become more intermittent and the mean velocities vanish at γ_c. At γ_c the system is both highly compressible and easily sheared. Finally, the typical stress chain length and orientation and the stress distributions change significantly as $\gamma \rightarrow \gamma_c^+$. In the space available, we demonstrate several of these properties; more details will be given elsewhere [12].

As sketched in Fig. 1, the apparatus consisted of an inner shearing wheel (A) (radius 10.34 cm) and an outer shearing ring (B) (inner radius 19.14 cm) confined by planetary gears (C). The apparatus was placed in a polarimeter using a circular polarization scheme [10]. The disks (D) (thickness = 6 mm) were confined between the wheel and ring as well as two smooth slippery horizontal Plexiglas sheets. (The friction between the disks and sheet was more than 2 orders of magnitude smaller than the typical force in a strong stress chain.)   We used a bimodal distribution of ~400d = 0.9 cm disks and ~2500d = 0.74 cm disks to avoid crystallization effects. We have checked for segregation by size and found that this does not occur to any measurable extent. The side of the wheel and the inner surface of the ring were coated with plastic "teeth" spaced 0.7 cm apart and 0.2 cm deep to enhance shearing. Although both the wheel and the outer ring could be used to shear, we focus here on shearing only with the inner wheel. The disks had a nominal Young's modulus, $E = 4.8$ MPa; the Plexiglas shearing wheel and ring had a nominal Young's modulus $E \simeq 3$ GPa. Each disk had a small dark bar which we used to track the position and orientation of individual disks using conventional video. We varied the packing fraction, γ, over the range $0.77 \leq \gamma \leq 0.81$. As we varied γ, we maintained the ratio of small to large disks as closely as possible to constant. The range of γ was chosen so that near the lower end, stress chains in a given region appeared only intermittently, and at the higher end, much of the system was continually filled with a high density of chains. Notably, only a small variation in γ, ~4%, was sufficient to traverse this regime. We varied the rotational rate, Ω, of the inner wheel over

the range $3.1 \times 10^{-3} \leq \Omega \leq 5.3 \times 10^{-2}$ rad/s. Data for such quantities as V_θ, the mean azimuthal velocity of the disks, are essentially independent of Ω (rate independent) [11], and we present V_θ in the scaled form V_θ/Ω.

Light rays passing through the polarimeter/apparatus along the axial direction of the disks have a transmitted intensity, $I \propto \sin^2(\theta)$, where $\theta \propto \sigma_2 - \sigma_1$. Here, the σ_i are the local planar principal stresses. Near a contact, the stresses within a disk are very nonuniform, which leads to a series of bands in the polariscope image, with the number of bands increasing monotonically with the force at the contact. We exploited this fact to produce a force calibration in terms of $G^2 \equiv |\nabla I|^2$, since the mean $\langle G^2 \rangle$ over the scale of a disk grows with the contact forces. We obtained this calibration (Fig. 3 inset) by applying known forces F to the boundary of a small number of disks (50–300) and at the same time measuring $\langle G^2 \rangle$. This technique is ultimately limited at very large stresses (larger than those typically encountered here) only by digital image resolution, and at very low stresses because the image across a single grain does not show a very large intensity gradient.

Before beginning to take data, we typically ran the inner wheel for ~60 min corresponding to ~20 rotations of the inner wheel. This allowed the mean density profile—more dilated near the wheel due to the shear band—to evolve. In addition, the mean velocity profile evolved as well, to a steady state that is well described by the form $\exp(-ar^2 + br)$, where r is the distance from the inner wheel [11].

We now demonstrate quantitatively some of the key properties near the ST. V_θ decreases with decreasing γ and vanishes at γ_c, as in Fig. 2. We demonstrate this explicitly in the inset in Fig. 2. This shows scaled data $V_\theta^* = (V_\theta/\Omega)/[(\gamma - \gamma_c)/\gamma_c]$ vs a weakly rescaled radial coordinate $r^* = r[1 + A(\gamma - \gamma_c)/\gamma_c]$ where $A = -12.70 \pm 0.7381$. A good collapse of the data, within the
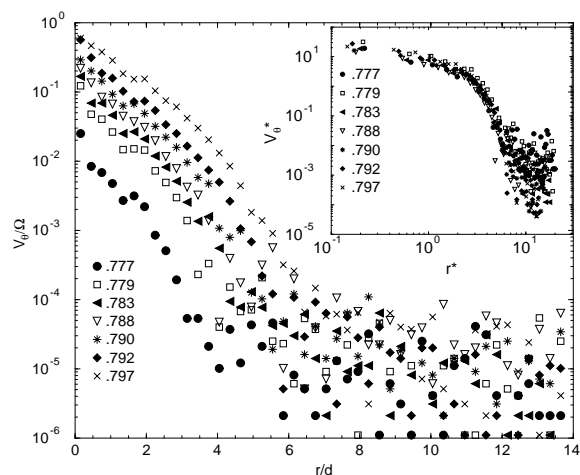

FIG. 2. Mean angular speed of disks normalized by the shearing rate, Ω, V_θ/Ω, vs distance r from the shearing wheel for various γ's, showing critical slowing down. Inset: Scaled data showing collapse.

scatter, results. The precise experimental determination of γ_c is difficult, because of the slow relaxation of transients. There is also another slow relaxation effect that is present at any γ: the velocity profile varies roughly exponentially with distance from the wheel, leading to slow relaxation in the outer portion of the sample.

The qualitative properties of stress distributions and temporal variations of the stress all change significantly with γ. We show at the bottom of Fig. 1 time series data for the force per disk obtained from G^2 integrated over $1/10$ of the system, for two different values of γ. Slightly above γ_c (lower trace), there are fractionally large intermittent positive variations in G^2 about a low mean value; at higher γ (upper trace) the mean stress is large, and there are fluctuations about this mean. Note that as $\gamma \to \gamma_c^+$, the time between fluctuations becomes large, whereas the time for a fluctuation to actually occur is set chiefly by Ω. Manifestly, the mean stress, $\bar{\sigma}$, vanishes at γ_c. Within the resolution of our experiments, $\bar{\sigma} \to 0$ continuously, as $\gamma \to \gamma_c^+$ (Fig. 3). Conversely, $\bar{\sigma}$ grows faster than exponentially in $(\gamma - \gamma_c)/\gamma_c$; this strengthening is at the heart of Reynolds dilatancy.

Power spectra, $P(f)$, for the time series such as those in Fig. 1 typically have the form of two power laws, one with $P(f) \propto f^{-2}$ at high frequencies, f, and the other with, $P(f) \propto f^{-\alpha}$, for low f, where $0 < \alpha < 2$. The qualitative shape of these spectra, to be discussed elsewhere, is similar to that found for 3D stress measurements [4].

We consider the force distributions $P(F)$ in Fig. 4. In this figure, the bottom set gives the distribution by averaging G^2 over a size comparable to one disk; the top set gives the force/disk found by averaging over ~260 disks collectively. For moderate γ, the 1-disk distribu-

tions are described at higher stresses by exponentials: $P \propto \exp(-F/F_o)$. For example $F_o = 0.173 \pm 0.004$ and 0.103 ± 0.004 for $\gamma = 0.777$ and 0.779, respectively. As γ is increased the distributions show a clear transition from approximately exponential variation with F when γ is moderate, to more nearly Gaussian for larger γ. Differences between these distributions provide a rough measure of correlations; i.e., for the case of forces that are uncorrelated from grain to grain, the distribution for N grains should narrow by $N^{-1/2}$ relative to the 1-disk distributions of the same γ. Narrowing is evident for larger γ, but not for $\gamma \simeq \gamma_c$.

It is also visually obvious [12] that close to γ_c, the stress network consists of long uninterrupted chains which tend to be oriented primarily radially and propagate much of the distance between the inner and outer wheel. But as γ increases, the network becomes more tangled, with many shorter intersecting chains, not necessarily radially oriented, as in Fig. 1, which has $\gamma \simeq 0.81$. This is intuitively reasonable, since as the disks are compressed, those bearing the largest forces will deform, so that other disks can carry some of the load. We estimated the distribution of chain lengths as a function of γ, and from these distributions we calculated the mean chain length, $\bar{L}$, as shown in Fig. 5. We defined the length of a chain to be any set of nearly collinear disks carrying stress larger than the mean. Using this definition, chains ended at branches
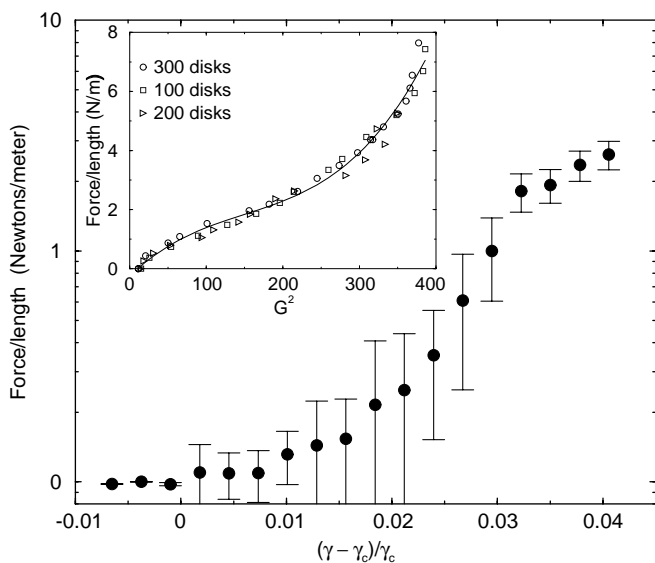

FIG. 3. Mean stress for ~260 disks vs $(\gamma - \gamma_c)/\gamma_c$ where $(\gamma_c \simeq 0.776)$. Inset: Calibration of $\langle G^2 \rangle$ vs applied normal force/unit boundary length for various numbers of particles. Force/length varies faster than exponentially in $\gamma - \gamma_c$ for the range of our experiments.
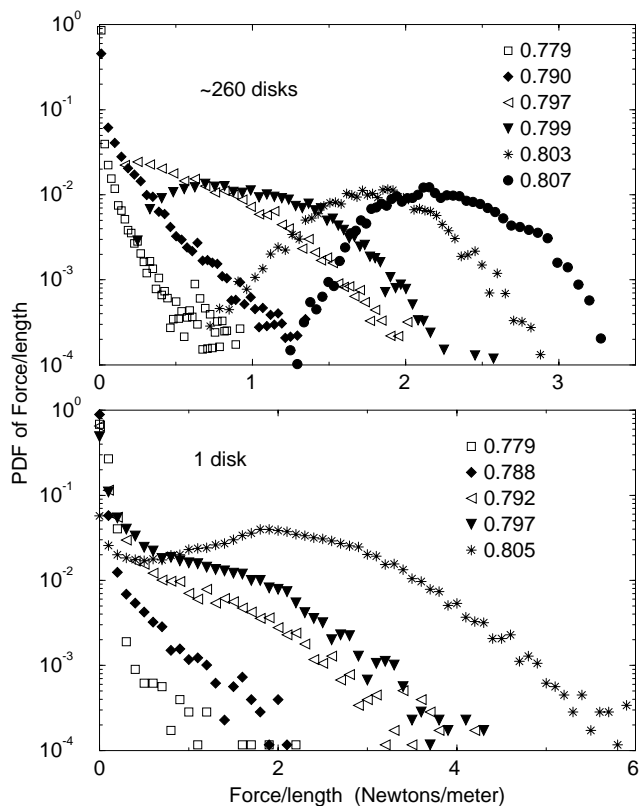

FIG. 4. Distribution for various packing fractions, γ. Top: force per particle for collections of ~260 particles at a time; bottom: for one particle at a time.
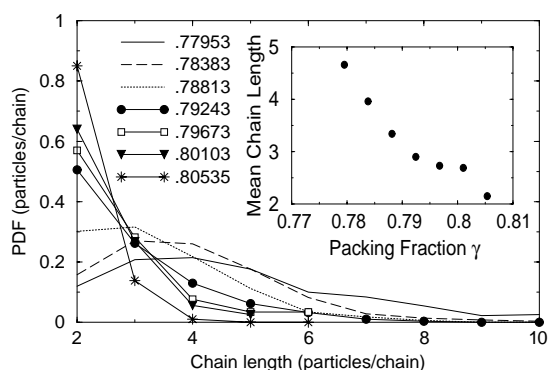
FIG. 5. Distributions of chain lengths L for the indicated γ. Inset: Mean chain length $\bar{L}$ vs γ.

in the stress lines, or at boundaries. We note that this definition is somewhat *ad hoc*. However, a more rigorous one is quite difficult to implement from the current experimental data. $\bar{L}$ grows (although it does not necessarily diverge) as $\gamma \to \gamma_c^+$. We believe that the length of the chains is roughly inversely related to the rigidity of the system. Near γ_c, chains are unstable to buckling, unless they are nearly perfectly aligned, and supported at their ends by the solid boundaries. For higher γ, the chains are better supported against buckling, and as noted above, more contacts can carry the applied load. For a highly compacted system, almost all of the contacts are actively carrying force, and the system looks more homogeneous.

To conclude, we have identified a well defined transition, the strengthening/softening transition that occurs as γ is varied through γ_c. The transition at γ_c shows a number of key features that include (1) an order parameter (the mean stress), (2) slowing down of velocities through increasingly intermittent displacement of disks, (3) large compressibility, (4) change in character of stress chains, including an increase in their mean length, and (5) qualitative changes in statistical properties such as the force distribution. With increasing γ, the system becomes more homogeneous. It seems possible that the transition exists more broadly, i.e., in 3D systems of nonrigid particles, since the qualitative reasons for its occurrence—a minimum packing fraction below which shearing does not occur—is a universal property for all granular systems. Ordinarily, however, gravity obscures this transition, and for completely rigid particles in a rigid container, the transition is not likely to be continuous. We note that the present system is small, and an important goal for future work is the investigation of larger systems. Equally important is the development of new techniques to facilitate a determination of the spatial character of the stress chains.

[1] For a broad review, see H. M. Jaeger, S. R. Nagel, and R. P. Behringer, Phys. Today **49**, No. 4, 32 (1996); (to be published); *Physics of Granular Media,* edited by D. Bideau and J. Dodds, Les Houches Series (Nova, Commack, NY, 1991); *Granular Matter: An Interdisciplinary Approach,* edited by A. Mehta (Springer, New York, 1994); R. P. Behringer, Nonlinear Sci. Today **3**, 1 (1993).

[2] P. Dantu, Géotechnique **18**, 50 (1968); A. Drescher and G. De Josselin De Jong, J. Mech. Phys. Solids **20**, 337 (1972); T. Travers *et al.,* J. Phys. A **19**, L1033 (1986).

[3] G. W. Baxter and R. P. Behringer, Eur. J. Mech. B **10**, 181 (1991); C. H. Liu and S. R. Nagel, Phys. Rev. Lett. **68**, 2301 (1992); G. W. Baxter, R. Leone, and R. P. Behringer, Europhys. Lett. **21**, 569 (1993); A. Ngadi and J. Rajchenbach, Phys. Rev. Lett. **80**, 273 (1998); Daniel K. Mueth *et al.,* Phys. Rev. E **57**, 3164 (1998).

[4] B. J. Miller, C. O'Hern, and R. P. Behringer, Phys. Rev. Lett. **77**, 3110 (1996).

[5] R. Jackson, in *Theory of Dispersed Multiphase Flow,* edited by Richard E. Meyer (Academic Press, New York, 1983), p. 291; R. M. Nedderman, *Statics and Kinematics of Granular Materials* (Cambridge University Press, Cambridge, England, New York, 1992).

[6] C.-h. Liu, S. R. Nagel, D. A. Schecter, S. N. Coppersmith, S. Majumdar, O. Narayan, and T. A. Witten, Science **269**, 513 (1995); S. N. Coppersmith, C.-h. Liu, S. Majumdar, O. Narayan, and T. A. Witten, Phys. Rev. E **53**, 4673 (1996).

[7] Phillipe Claudin and Jean-Phillipe Bouchaud, Phys. Rev. Lett. **78**, 231 (1997); Christophe Eloy and Eric Clément, J. Phys. I (France) **7**, 1541 (1997); Mario Nicodemi, Phys. Rev. Lett. **80**, 1340 (1998); Joshua E. S. Socolar, Phys. Rev. E **57**, 3204 (1998).

[8] F. Radjai, M. Jean, J.-J. Moreau, and S. Roux, Phys. Rev. Lett. **77**, 274 (1996).

[9] Photoelastic disks made from polymer PSM-4 obtained from The Measurements Group Inc.

[10] R. B. Heywood, *Designing by Photoelasticity* (Chapman and Hall Ltd., London, 1952).

[11] D. Howell *et al.,* in *Proceedings of the Workshop on Friction, Arching and Dilatancy,* edited by E. E. Wolf and P. Grassberger (World Scientific, Singapore, 1997); C. T. Veje *et al.,* in *Physics of Dry Granular Media,* edited by Hans J. Herrmann, J.-P. Hovi, and S. Luding, Nato ASI, Ser. E, Vol. 350 (Kluwer Academic, Dordrecht, Boston, 1998); Phys. Rev. E **59**, 739 (1999).

[12] D. Howell, C. Veje, and R. Behringer (to be published).